

## Isospin-symmetry violating branch of $^{42}\text{Sc}$ $\beta^+$ decay

A. M. Sandorfi, C. J. Lister, D. E. Alburger, and E. K. Warburton

Brookhaven National Laboratory, Upton, New York 11973

(Received 19 June 1980)

The branching fraction of the  $^{42}\text{Sc}$   $0^+$  ground state to the  $0^+$  1837-keV level of  $^{42}\text{Ca}$  was determined to be  $(1.03 \pm 0.31) \times 10^{-4}$  relative to the superallowed decay to the  $0^+$   $^{42}\text{Ca}$  ground state. The experiment was designed to eliminate possible spurious effects and systematic errors. Our result overlaps the larger of two recent measurements which were in rather poor agreement, and is half of that predicted by current microscopic calculations. The importance of this measurement in the extraction of the vector coupling constant  $G_V$  is discussed.

[RADIOACTIVITY  $^{42}\text{Sc}$ (g.s.); measured  $\beta^+$ -decay branch to the  $^{42}\text{Ca}$   $0^+$  1837-keV level.]

### I. INTRODUCTION

Superallowed  $\beta$  decays between  $0^+$  analog states have long played a crucial role in testing fundamental concepts.<sup>1,2</sup> One of these is the conserved vector current (CVC) hypothesis that such transitions should have a constant  $ft$  value, after small electromagnetic corrections. A "best"  $ft$  value, extracted from these superallowed decays assuming CVC, yields a weak-interaction-vector-coupling constant  $G_V$ . Comparing this value of  $G_V$  to that extracted from muon decay yields information on such fundamentals as the structure of the nucleon.<sup>2</sup>

A very important obstacle to be overcome in the extraction of  $G_V$  from nuclear  $\beta$  decay is the evaluation of the small effects of isospin-symmetry breaking by Coulomb and nuclear forces. These effects give rise to  $T_3$ -dependent distortions which mix wave functions of other nuclear states differently into the initial and final states, and cause a mismatch between the initial and final wave functions in a superallowed  $0^+ \rightarrow 0^+$  transition. Levels with isospin  $T$  different from that of the initial and final states will be mixed in, but the important admixtures are of other states of the same  $T$ . The status of attempts to calculate this effect has been discussed by Wilkinson<sup>2</sup> in a recent comprehensive review of  $\beta$  decay and related problems.

For a  $0^+ \rightarrow 0^+$  transition between  $T=1$  states the Fermi matrix element is

$$|M_V^0|^2 = 2(1 - \delta) \approx 2(1 - \delta_1)(1 - \delta_2), \quad (1a)$$

where  $\delta$  is the mismatch factor due to the  $T_3$ -dependent mixing.<sup>2,3</sup> It is customary<sup>3,4</sup> to split  $\delta$  into two parts as shown. The term in  $\delta_1$  arises from charge dependent configuration mixing with excited  $0^+$  states while the other factor  $(1 - \delta_2)$

arises from the difference between the radial wave function of the nucleon making the transition—a proton in one state and a neutron in the other—which leads to a radial overlap less than unity. As pointed out by Towner, Hardy, and Harvey,<sup>3</sup> whom we follow here, this separation is not rigorously allowed. However, it does lend itself to the perturbative treatments made to date.<sup>5</sup>

Current estimates<sup>2-4</sup> of  $\delta_2$  predict it to dominate with values between 0.2–0.9% for  $14 < A < 60$ , with  $\delta_1$  some 3–5 times smaller. The recent attempts<sup>2</sup> to obtain nucleon-structure information from the 2% difference between the vector coupling constants of nuclear  $\beta$  decay and muon decay illustrate the importance of checking the theoretical estimates for  $\delta$  whenever possible. The values of  $\delta_2$  for most nuclei are probably adequately represented by recent calculations,<sup>3</sup> but the estimates for  $\delta_1$  are strongly model dependent.<sup>2-5</sup>

A favorable opportunity for checking the calculation of  $\delta_1$  is offered by the presence in  $^{42}\text{Ca}$  of a  $0^+$  state only 1837 keV above the  $0^+$  ground state as illustrated in Fig. 1.<sup>6</sup> Both of these  $T=1$   $0^+$  states are energetically accessible to  $\beta^+$  decay from the  $^{42}\text{Sc}$   $T=1$   $0^+$  ground state. In the approximation that only the two lowest  $T=1$   $0^+$  states mix, in both  $^{42}\text{Sc}$  and  $^{42}\text{Ca}$ , the Fermi matrix element for the transition to this excited  $0^+$  in  $^{42}\text{Ca}$  may be written as

$$|M_V^1|^2 = 2\delta_1(1 - \delta_2). \quad (1b)$$

[The factor  $(1 - \delta_2)$  appearing here—the radial overlap correction for the  $^{42}\text{Sc}$   $0^+$  ground state and  $^{42}\text{Ca}$   $0^+$  excited state—is actually different from that of Eq. (1a) above, but to leading order such differences may be neglected.] The diminution of the ground-state decay by a branch to the 1837-keV level is then directly proportional to  $\delta_1$ .

The importance of a measurement of the  $\beta^+$ -decay branch of  $^{42}\text{Sc}$  to the  $^{42}\text{Ca}$  1837-keV level has been recognized since the first attempts to measure it.<sup>7-10</sup> However, only recently have the repeated attempts to detect this branch yielded positive results. Ingalls, Overley, and Wilson<sup>11</sup> obtained a branching ratio (BR) relative to the ground-state transition of  $(6.2 \pm 2.6) \times 10^{-5}$ , while DelVecchio and Daehnick<sup>12</sup> obtained  $(2.2 \pm 1.7) \times 10^{-5}$ . There are a few points of concern that may account for this discrepancy. In both of these measurements the  $^{42}\text{Sc}$  ground state was formed via  $^{42}\text{Ca}(p, n)^{42}\text{Sc}$  and a search was made for the ground state decay of the 1524-keV first-excited state of  $^{42}\text{Ca}$  to which the 1837-keV  $0^+$  state decays some 98% of the time (see Fig. 1). In the measurement of Ingalls *et al.*, a contaminant  $\gamma$  ray of 1523.8 keV was formed from the  $(p, n)$  reaction on the Pb backing of the  $^{42}\text{Ca}$  target. Its intensity amounted to  $(34 \pm 6)\%$  of the observed 1524-keV yield. Furthermore, although Ingalls *et al.* stored data in four 0.5 s time bins, they did not report to what extent the intensity of the 1524-keV  $\gamma$  ray followed the expected 0.68 s half-life of  $^{42}\text{Sc}$ . Finally, the result of DelVecchio and Daehnick is not very significantly different from

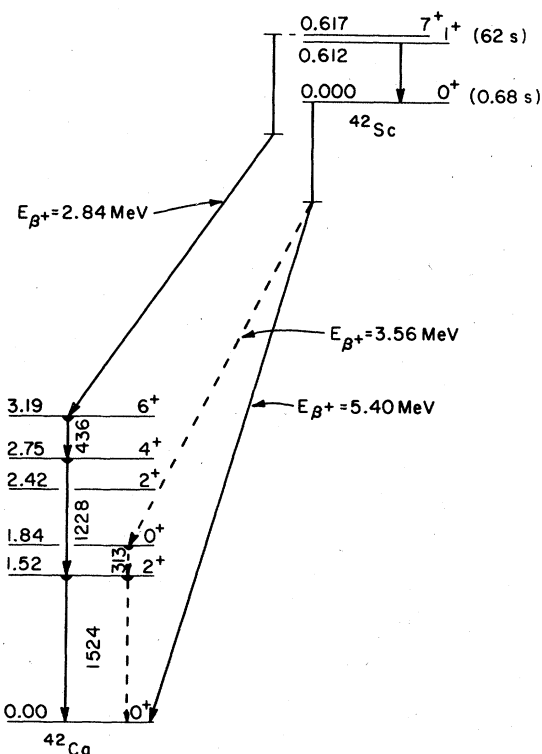


FIG. 1. The decay scheme of  $^{42}\text{Sc}$  is shown here together with the transitions (in keV) within the daughter nucleus  $^{42}\text{Ca}$  that are relevant to this work.

zero—in fact, they interpreted it as an upper limit,  $\text{BR} < 3.9 \times 10^{-5}$ —and is in rather poor agreement with that of Ingalls *et al.* In order to put this important branching ratio on more firm experimental ground, we undertook a new measurement designed to eliminate as many spurious effects and systematic errors as possible.

## II. EXPERIMENTAL GEOMETRY

We have used the  $^{42}\text{Ca}(p, n)$  reaction to produce  $^{42}\text{Sc}$ . The  $Q$  value for this reaction is  $Q = -7.206$  MeV,<sup>6</sup> and incident proton energies less than 8.009 MeV will excite the  $^{42}\text{Sc}$  ground state without exciting the  $7^+$  state at 0.617 MeV which also  $\beta^+$  decays back to  $^{42}\text{Ca}$  (see Fig. 1). The targets, films of 94% isotopically-enriched  $^{42}\text{Ca}$  ranging in thickness from 0.7 to 1.6 mg/cm<sup>2</sup>, were evaporated onto 0.025-mm gold foils and covered with a coating of 200  $\mu\text{g}/\text{cm}^2$  of gold to reduce oxidation and increase durability. The proton beam passed through a 1-mg/cm<sup>2</sup> nickel foil ( $\Delta E_p = 34$  keV) and an equivalent of 200  $\mu\text{g}/\text{cm}^2$  of He gas ( $\Delta E_p = 4$  keV) before striking one of these targets, clamped in a plastic holder or "rabbit." An average of 0.5  $\mu\text{A}$  of 8.000-MeV protons, 42 keV below threshold for production of an excited state of  $^{42}\text{Sc}$ , was used throughout the search for isospin-symmetry-breaking decays. Using the BNL-target-transport system,<sup>13</sup> the rabbit was cycled between the bombardment position and a shielded-remote-counting station 5 m away to reduce the high rate of prompt decay radiation.

Previous attempts at detecting the  $\beta^+$  decay of  $^{42}\text{Sc}$  to the 1837-keV level in  $^{42}\text{Ca}$  have used the 1524-keV  $\gamma$  decay from the first excited state in  $^{42}\text{Ca}$  as a signature for this  $\beta^+$  transition<sup>7-12</sup> (see Fig. 1). The use of a rabbit-transport system removes the high yield of reaction  $\gamma$  rays, and the remaining chief sources of background have been either from  $\beta^+$  annihilation in flight or from other contaminant  $\gamma$  rays, such as the 1157-keV transition arising from the decay of  $^{44}\text{Sc}$  to  $^{44}\text{Ca}$  which, when summed with a 511-keV annihilation signal, can produce yield in the vicinity of 1524 keV.<sup>11, 12</sup>

Our measurement was designed to enhance the signal for  $\beta^+$  decay to the 1837-keV level in  $^{42}\text{Ca}$  relative to the background by demanding a triple coincidence between a 511-keV  $\gamma$  ray from stopped  $\beta^+$  annihilation, the 313-keV  $\gamma$  ray resulting from the  $0_2^+ \rightarrow 2_1^+$  transition in  $^{42}\text{Ca}$ , together with the final  $2_1^+ \rightarrow 0_1^+$  1524-keV transition from the first excited state in  $^{42}\text{Ca}$  to the ground state. After a bombardment cycle the rabbit system transported the decaying  $^{42}\text{Sc}$  sample to the center region of a 25.4-cm diameter by 20.3 cm deep cylindrical NaI(Tl) crystal through one port of a T-shaped

cavity, as shown in Fig. 2. The NaI(Tl) crystal is split into two halves that are optically isolated and each viewed by 2 photomultiplier tubes (RCA-4900). The plane of optical isolation contained the rabbit transport tube. In the region of the counting position the rabbit is surrounded by 1 cm of graphite which is used to moderate the positrons. The cavity running the length of the crystal perpendicular to the rabbit line is actually off center so that the NaI(Tl) is only 4.5 cm thick near the rabbit entrance hole. As shown in Fig. 2, two additional 12.7-cm diameter NaI(Tl) crystals were used to increase the effective detector wall thickness in this region. The negative-high-voltage levels on the 3 photomultiplier tubes viewing each

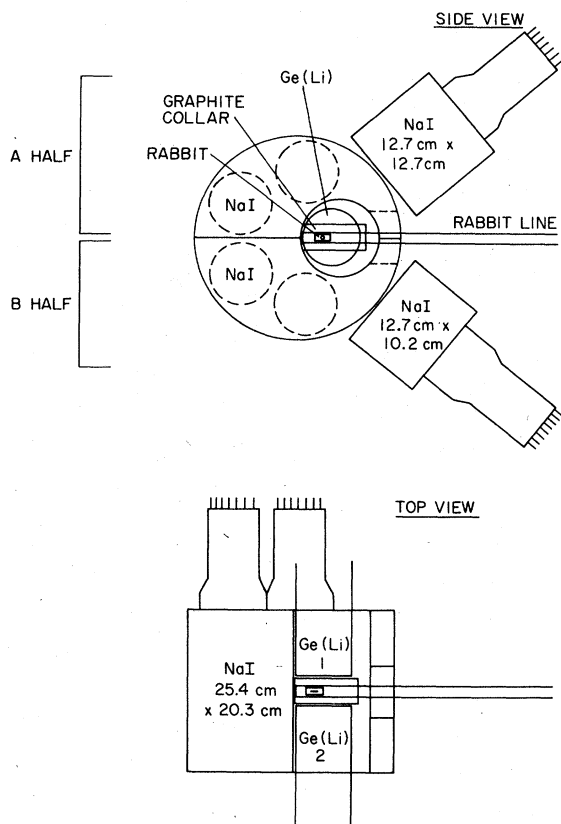


FIG. 2.  $^{42}\text{Sc}$  nuclei, produced in the reaction  $^{42}\text{Ca}(p, n)^{42}\text{Sc}$ , were cycled to a remote counting station shown here schematically. The rabbit line entered through one port of a T-shaped cavity in a cylindrical NaI(Tl) detector that is split into two optically isolated halves, the position of the rabbit coinciding with the plane of optical isolation. The cavity running the length of the NaI(Tl) crystal is off center and the NaI(Tl) detector thickness was augmented by two 12.7-cm-diam crystals, as shown. Two Ge(Li) detectors were positioned within the NaI(Tl) cavity abutting a graphite collar that surrounded the rabbit. (See text for further discussion.)

“half” of the NaI(Tl) detector—two on the semi-annular segment and one on an additional 12.7-cm crystal—were adjusted to provide the best summed-pulse-height resolution [about 12% full width at half maximum (FWHM)] for 511-keV  $\gamma$  rays from a  $^{22}\text{Na}$  source mounted on a rabbit and situated in the count position. Transistor stabilization at the last four dynodes of each tube reduced rate-dependent gain shifts to a negligible effect.<sup>14</sup> The summed anode signals from each half were clipped to a total width of 200 ns with an almost-shorter-delay line. Gamma-ray energy “windows” were placed directly on these summed anode signals. To ensure proper operation at high rates, fast (>100 MHz) constant-fraction discriminators were used to set the lower (with normal logic) and upper (with complementary logic) energy limits and a fast coincidence between these (resolving time = 50 ns) served to indicate the presence of a pulse of amplitude within the window. Windows on the 511-keV annihilation line were set up with a  $^{22}\text{Na}$  source. Whenever one 511-keV  $\gamma$  ray is detected in one half of the NaI(Tl) detector, the other 511-keV annihilation quantum has a very high probability of entering the other half, and so the 313-keV  $\gamma$  rays were actually detected by placing windows on the sum peak at 824 keV. To set these a  $^{54}\text{Mn}$  source was used, providing a line at 834.8 keV. A background window was set above this at 947 keV with a  $^{152}\text{Eu}$  source which provides a line at 964.1 keV. The final element of the triple coincidence, the 1524-keV  $\gamma$  ray, is sought in the spectra of two Ge(Li) detectors positioned within the NaI(Tl) cavities against the graphite absorber as shown in Fig. 2. The Ge(Li) spectra were gated by fast triple coincidences (resolving time of 20 ns) requiring a Ge(Li) signal accompanied by signals within two NaI(Tl) windows. Using the labeling of Fig. 2, the gates for the Ge(Li) spectra may be written as

$$(824)_A + (511)_B + \text{Ge(Li)}_1, \quad (2a)$$

$$(824)_B + (511)_A + \text{Ge(Li)}_1, \quad (2b)$$

$$(824)_A + (511)_B + \text{Ge(Li)}_2, \quad (2c)$$

$$(824)_B + (511)_A + \text{Ge(Li)}_2. \quad (2d)$$

Background spectra were collected gated by the requirements

$$\left. \begin{array}{l} [(947)_A + (511)_B] \\ \text{or} \\ [(947)_B + (511)_A] \end{array} \right\} + \text{Ge(Li)}_1 \quad (3a)$$

and

$$\left. \begin{array}{l} [(947)_A + (511)_B] \\ \text{or} \\ [(947)_B + (511)_A] \end{array} \right\} + \text{Ge(Li)}_2. \quad (3b)$$

(It is important to note that, apart from background considerations, a threefold coincidence requirement is necessary to keep the rate of accidental coincidences down to an acceptable level.) The singles spectra in the two Ge(Li) detectors were also collected to monitor the yield of 511-keV  $\gamma$  rays which was used to extract the number of  $^{42}\text{Sc}$  nuclei produced.

Out of every rabbit cycle, lasting 4.8 s, the  $^{42}\text{Ca}$  target was irradiated for 1.2 s (~two  $^{42}\text{Sc}$  half-lives) and the spectra of decay radiation was collected in the counting position of Fig. 2 for 1.6 s. During the counting period, the singles Ge(Li) spectra were collected in four time bins, each 0.4 s, so that the fast component of 511-keV  $\gamma$  rays could be extracted from longer lived decays. The rabbits were changed every four hours to reduce the yield from long-lived activities, such as  $^{44}\text{Sc}$ , that build up during the course of the measurement. In all, five different rabbits were used. The Ge(Li) spectra, gated by the triple coincidence requirements of Eq. (2) and Eq. (3) above, were collected in two time bins of 0.8 s each so that any long-lived contributions to the yield at 1524 keV could be removed.

### III. DETECTION EFFICIENCY

In the experimental setup described above, the NaI(Tl) is used as a filter for 1524-keV  $\gamma$  rays from  $\beta^+$  decays to the second  $0^+$  state (1837 keV) in  $^{42}\text{Ca}$ . With the complicated geometry of Fig. 2, the efficiency of this filter is extremely difficult to calculate. It can, however, be measured in a straightforward manner. At  $E_\beta > 8.009$  MeV, the  $\beta^+$  decay of the  $7^+$  isomeric state in  $^{42}\text{Sc}$  is followed by a 436–1228–1524 keV  $\gamma$ -ray cascade as indicated in Fig. 1. The 436-keV transition can be detected in one segment of the NaI(Tl) in place of the 313-keV line discussed above. Once again, if one 511-keV  $\gamma$  ray from stopped  $\beta^+$  annihilation is detected in one half of the NaI(Tl) detector, the other corresponding 511-keV  $\gamma$  ray will have a very high probability of entering the other half, and so the 436-keV peak would actually show up as a sum peak at 947 keV—which is just the energy appearing in the gates listed in Eq. (3) above. The efficiency of the NaI(Tl) filter for detecting a 511-keV  $\gamma$  ray and a lower energy  $\gamma$  ray is just the ratio of fourfold coincidences [1228-keV  $\gamma$  ray detected in one Ge(Li) and a 1524-keV  $\gamma$  ray detected in the other Ge(Li) along with 511- and 947-keV signals detected in opposite halves of the NaI(Tl)

array] to the number of twofold coincidences [1228-keV and 1524-keV  $\gamma$  rays detected in opposite Ge(Li) detectors]. Ge(Li) spectra were collected at  $E_\beta = 9.5$  MeV gated by the coincidence requirements in Eq. (3) above. The resulting efficiencies of the NaI(Tl) filter were  $0.074 \pm 0.004$  for Ge(Li)<sub>1</sub> and  $0.073 \pm 0.004$  for Ge(Li)<sub>2</sub>. In the actual measurement below the  $7^+$  threshold, the NaI(Tl) filter searches for 511- and 313-keV transitions. The absolute efficiency of the two NaI(Tl) sections was measured at 350 keV and 661 keV using calibrated  $^{133}\text{Ba}$  and  $^{137}\text{Cs}$  sources, respectively, mounted on rabbits in the count position. The fourfold to twofold ratios were then corrected for the increased efficiency at 313 keV vs 436 keV to yield the absolute efficiencies for the NaI(Tl) filter of  $0.083 \pm 0.004$  for Ge(Li)<sub>1</sub> and  $0.082 \pm 0.004$  for Ge(Li)<sub>2</sub>.

There are two further corrections to these efficiencies that are due to the difference between the  $\beta^+$  end-point energies in the efficiency measurement ( $E_\beta = 2.84$  MeV) and in the actual experiment below the  $^{42}\text{Sc}^{7+}$  threshold ( $E_\beta = 3.56$  MeV). First, there is a difference in the amount of positron annihilation in flight which effectively reduces the number of 511-keV  $\gamma$  rays available for detection in the NaI(Tl) filter. Gerhart, Carlson, and Sherr<sup>15</sup> have measured the total probability of annihilation in flight in Lucite of positrons from  $^{35}\text{Ar}$ ,  $E_\beta = 4.94$  MeV,<sup>6</sup> and from  $^{19}\text{Ne}$ ,  $E_\beta = 2.22$  MeV.<sup>16</sup> This effect is not strongly dependent upon the  $Z$  of the moderating medium,<sup>15</sup> and so assuming their values for Lucite are identical to the values for graphite, and interpolating linearly between their results, we obtain 0.045 and 0.050 for the total probability of annihilation in flight from  $\beta^+$  end-point energies of 2.84 MeV and 3.56 MeV, respectively. The efficiency of the NaI(Tl) filter, during the search for the weak branch to the 1837-keV level in  $^{42}\text{Ca}$ , must then be corrected down by  $\frac{1}{2}\%$  to

$$EF_1 = 0.082 \pm 0.004 \text{ for Ge(Li)}_1, \quad (4a)$$

and

$$EF_2 = 0.082 \pm 0.004 \text{ for Ge(Li)}_2. \quad (4b)$$

The second effect of the different  $\beta^+$  end-point energies arises from the difference in the extent of the 511-keV annihilation-emitting source. The effective range of 2.84- and 3.56-MeV positrons in graphite differs by 0.2 cm.<sup>17</sup> The further away the annihilation point is from the center line of the NaI(Tl) assembly, the greater the chance both 511-keV  $\gamma$  rays have of entering the same half of the NaI(Tl) array and defeating the action of the filter. With the geometry of Fig. 2, this effect is quite hard to calculate. However, we have ob-

tained a measure of it with a  $^{22}\text{Na}$  source, mounted on a rabbit in the counting position, by determining the efficiency of detecting both 511-keV  $\gamma$  rays from stopped  $\beta^+$  annihilation in opposite halves of the NaI(Tl) in coincidence with 1274-keV radiation observed in one of the Ge(Li) detectors. This efficiency—the ratio of triple coincidences to the singles yield of 1274-keV  $\gamma$  rays measured in the Ge(Li)—changed by 1% when the center line of the rabbit, transfer assembly, and graphite absorber was moved 1 cm below the plane of optical isolation in the NaI(Tl). From this we estimate that the corresponding correction to the efficiencies in Eq. (4) cannot be more than a few tenths of a percent and, considering the other errors involved, can be neglected in our analysis.

The branching ratio of interest is extracted by comparing the yield of 1524-keV  $\gamma$  rays observed through the NaI(Tl) filter at  $E_p = 8.000$  MeV to the total number of fast 511-keV annihilation quanta detected in the Ge(Li) counters, the latter being a measure of the  $^{42}\text{Sc}_{g.s.}(\beta^+)^{42}\text{Ca}_{g.s.}$  superallowed decay. However, this must be corrected for the difference in Ge(Li) detection efficiencies at 1524 and 511 keV. This difference was measured at  $E_p = 9.5$  MeV which, following the  $\beta^+$  decay of the  $^{42}\text{Sc}$   $7^+$  isomer, provided the 436–1228–1524 keV cascade of *equal intensity*  $\gamma$  rays. The use of constant fraction discriminators with slow-rise-time rejection improved the Ge(Li) timing characteristics but greatly suppressed the counting

efficiency below 600 keV with the resulting relative efficiencies:

$$\epsilon_1 = \frac{\epsilon_1(511)}{\epsilon_1(1524)} = 0.74 \pm 0.04 \text{ for Ge(Li)}_1, \quad (5a)$$

and

$$\epsilon_2 = \frac{\epsilon_2(511)}{\epsilon_2(1524)} = 1.35 \pm 0.02 \text{ for Ge(Li)}_2. \quad (5b)$$

[The risetime of the signals from Ge(Li)<sub>1</sub> changed substantially at lower energies, and this is reflected in Eq. (5a).]

Finally, the data at  $E_p = 9.5$  MeV provided copious quantities of 1524-keV  $\gamma$  rays which enabled accurate determination of both the calibration and line shape for the two Ge(Li) detectors at exactly the energy necessary for the isospin-symmetry-breaking  $\beta^+$ -decay search.

#### IV. DATA

The sum of the Ge(Li) spectra gated by the triple-coincidence requirements of Eq. (2) for the first half of the counting period (0.8 s) is shown in Fig. 3, and represents approximately 25 h of data at  $E_p = 8.000$  MeV. The 1157-keV line from the contaminant  $^{44}\text{Ca}$  is accompanied by two 511-keV annihilation quanta, one of which can be accidentally in coincidence with a lower energy  $\gamma$  ray in one half of the NaI(Tl). [The rates in the NaI(Tl) segments above 100 keV decayed from

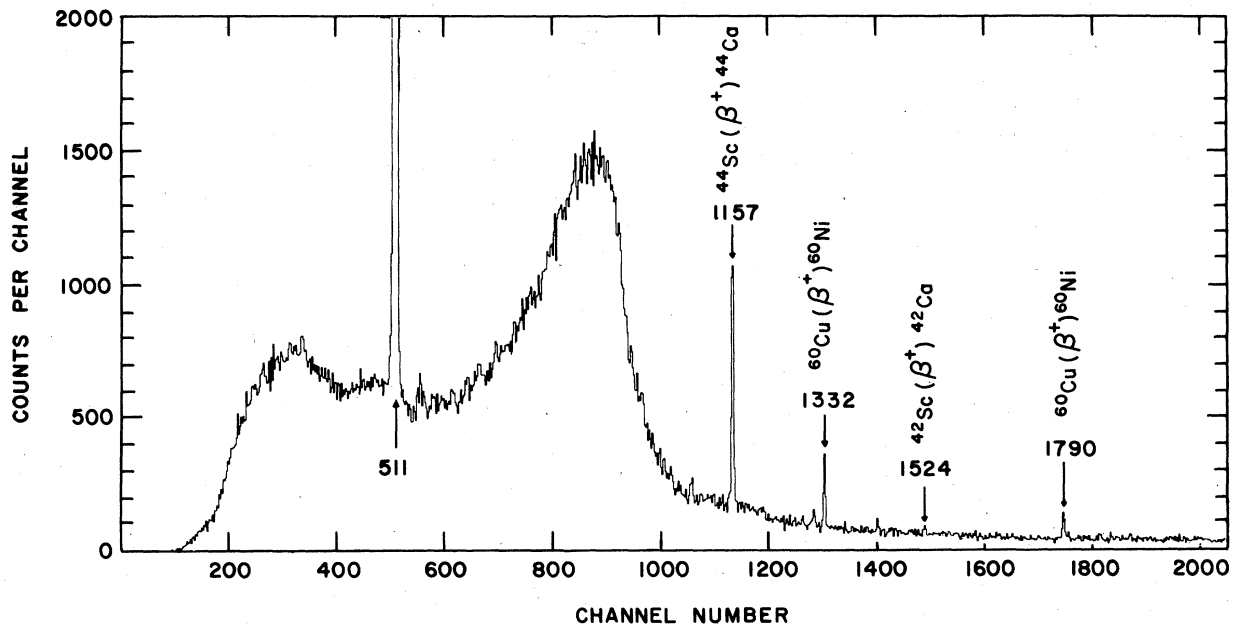


FIG. 3. The sum of the triple-coincidence Ge(Li) spectra obtained at  $E_p = 8.000$  MeV during the first 0.8 s of the counting period is shown here. The prominent  $\gamma$ -ray transitions are labeled by their energies in keV. The sources of these lines are indicated and are further discussed in Sec. IV.

100 to 25 KHz during the counting period, while those in the Ge(Li) detectors decayed from 12 to 5 KHz.] Alternatively, the 1157-keV  $\gamma$  ray can Compton scatter in one half of the NaI(Tl) and fulfill the requirements of the filter while a 511-keV  $\gamma$  ray is detected in a Ge(Li). Such effects account for the presence of these lines in the triple-coincidence spectrum of Fig. 3. The large broad peak some 313 keV below the energy of the 1157-keV line is just an image of the gate in Eq. (2) which is satisfied by Compton scattering of an 1157-keV  $\gamma$  ray from a Ge(Li) into the NaI(Tl) with just the right energy so that the sum with a 511-keV signal will fall within the 824-keV window. The lines at 1332 and 1790 keV satisfy the coincidence requirements in a similar manner and arise from a ( $p,n$ ) reaction in the nickel window in front of the rabbit which then imbeds  $^{60}\text{Cu}$  into the target. These effects produce backgrounds which are constant throughout the 1.6 s counting interval.

The summed triple-coincidence Ge(Li) spectra obtained in the first and second halves of the counting period are shown in Figs. 4(a) and 4(b), respectively, for the region around 1524 keV. [Fig. 4(a) is an exploded view of Fig. 3 in the vicinity of the 1524-keV line.] The peak in channel 1489 clearly decays with a short half-life. Fitting these data to a 0.68 s exponential decay plus constant background yields an initial intensity at the start of the counting period of  $128 \pm 39$  events. As an alternate method for extracting the 1524-keV intensity, we fixed Gaussian line shape parameters from the 1524-keV photopeak observed at  $E_p = 9.5$  MeV (see Sec. III) and fitted this shape to the data from the sum of both halves of the counting period, stepping the centroid from channel to channel allowing only the area to vary. The results of this procedure are shown in Fig. 5. The largest area is obtained with the centroid in channel 1489, corresponding to 1524.3 keV. The total area of  $88 \pm 20$  counts in the 1.6 s counting interval corresponds to an initial intensity of  $113 \pm 26$  decays. In the analysis to follow we take the observed intensity as the mean of these two techniques:

$$Y_{\text{TOT}}(1524) = 120 \pm 33. \quad (6)$$

The summed background spectra, gated by the coincidence requirements in Eq. (3), are shown in Fig. 4(c) for the first half of the counting period. The NaI(Tl) discriminator windows for these events overlapped the 511–824-keV windows by about 10%. The yield in Fig. 4(c) has a contribution of 0.68 s 1524-keV  $\gamma$  rays which corresponds to 8% of the intensity observed in Fig. 4(a).

The number of superallowed  $\beta^+$  decays to the

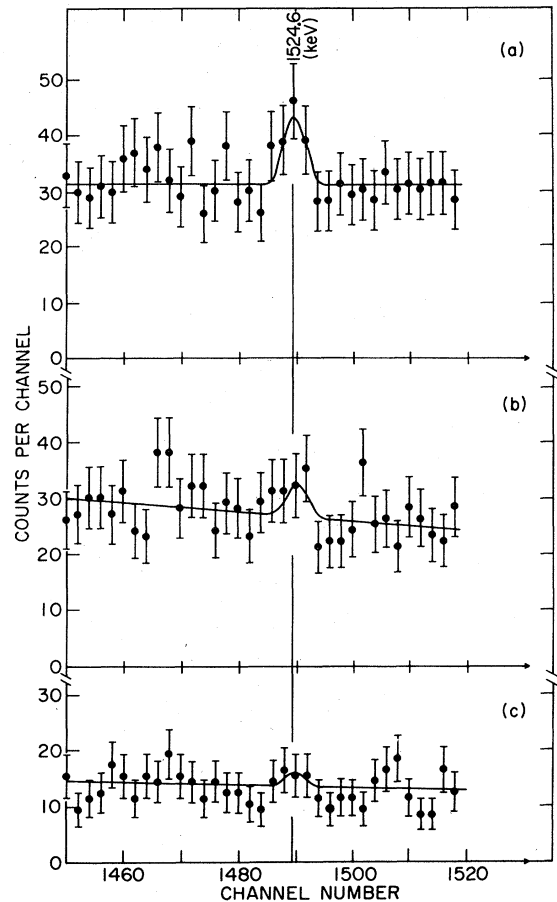


FIG. 4. The summed Ge(Li) spectra in the vicinity of 1524 keV, obtained at  $E_p = 8.000$  MeV in the first and second 0.8 s halves of the counting period, are shown in (a) and (b) gated by the triple-coincidence requirements of Eq. (2). The sum of the background spectra obtained in the first half of the counting period, gated by the requirements of Eq. (3), is shown in (c). The solid line through the data results from fits to a linear background plus a Gaussian with centroid and line shape parameters fixed by the 1524-keV photopeak observed at  $E_p = 9.500$  MeV. (The linear background was determined by a much larger portion of the spectra than evident here.) The vertical line marks the expected position of the  $2_1^+ \rightarrow 0_1^+$  transition in  $^{42}\text{Ca}$  (Ref. 6).

$^{42}\text{Ca}$  ground state that accompanied the data of Fig. 4 was extracted from the two Ge(Li) singles spectra which were collected in four 0.4 s time bins during the counting period (see Sec. II). The background-subtracted intensity of 511-keV  $\gamma$  rays was extracted for each time bin, and the four values were fitted to a 0.68 s exponential decay plus constant background. (Only data for which the short-lived component exceeded 50% of the 511-keV yield are presented in this paper.) From this, the number of 511-keV  $\gamma$  rays from the 0.68

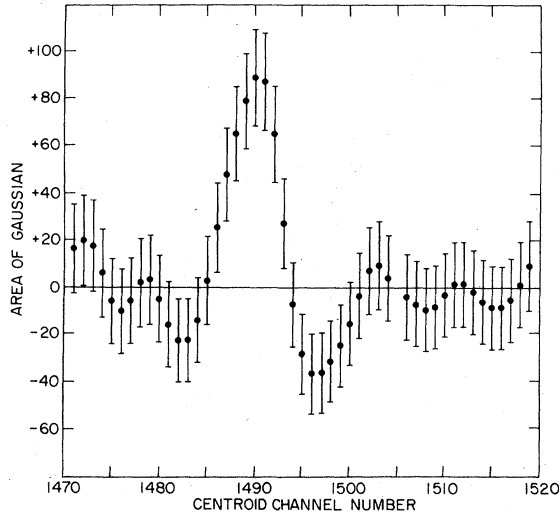


FIG. 5. The results of a Gaussian fit to all of the data at  $E_p = 8.000$  MeV are shown here. The line shape parameters were held fixed by the 1524-keV photopeak observed at  $E_p = 9.500$  MeV and the centroid was stepped from channel to channel allowing only the area to vary. This technique is particularly sensitive to distinguishing real photopeaks from statistical fluctuations of the background.

s decay of  $^{42}\text{Sc}$  was found to be

$$Y_1(511) = 1.087 \pm 0.054 \times 10^7 \text{ in Ge(Li)}_1, \quad (7a)$$

and

$$Y_2(511) = 1.883 \pm 0.094 \times 10^7 \text{ in Ge(Li)}_2. \quad (7b)$$

#### V. DETERMINATION OF THE BRANCHING RATIO

The branching ratio (BR) of decays from the  $^{42}\text{Sc}$   $0^+$  ground state to the  $0^+$  1837-keV level of  $^{42}\text{Ca}$  relative to the superallowed decay to the  $0^+$   $^{42}\text{Ca}$  ground state, as determined by the data from the first Ge(Li) detector, can be written as

$$\text{BR} = \frac{Y_1(1524)}{1/2Y_1(511)} \frac{\epsilon_1}{EF_1}. \quad (8)$$

In order to minimize the error in the face of poor statistics it is better to perform a single determination of BR from the combined data of both Ge(Li) detectors. If Eq. (8) is rewritten for the second Ge(Li) detector, and if these two equations are then added, one obtains an expression for the combined 1524-keV yield extracted from Figs. 4 and 5, as discussed in Sec. IV above. This then gives the branching ratio as

$$\text{BR} = \frac{2Y_{\text{TOT}}(1524)\epsilon_1\epsilon_2}{Y_1(511)\epsilon_2EF_1 + Y_2(511)\epsilon_1EF_2}. \quad (9a)$$

Combining Eqs. (4), (5), (6), and (7) then gives  $(1.02 \pm 0.31) \times 10^{-4}$  for the branching fraction. The yield of 1524-keV  $\gamma$  rays seen through the NaI(Tl) filter, Eq. (6) above, is proportional to the number of 511-keV  $\gamma$  rays from stopped 3.56-MeV  $\beta^+$  annihilation. However, the yield of 511-keV  $\gamma$  rays in the denominator of Eq. (9a), proportional to the number of superallowed decays and given by Eq. (7), is really the yield of stopped 5.40-MeV  $\beta^+$  annihilation. As discussed in Sec. III, the number of 511-keV  $\gamma$  rays is reduced by the probability of annihilation in flight—0.050 and 0.063 for 3.56-MeV and 5.40-MeV positions, respectively. This lowers the branching ratio by 1.2%. Correcting for  $e^+e^-$  pair emission from the 1837-keV state<sup>18</sup> then raises BR by  $(2.05 \pm 0.17)\%$  to give our final result

$$\text{BR} = (1.03 \pm 0.31) \times 10^{-4}. \quad (9b)$$

Contributions to the 1524-keV yield from second-forbidden  $^{42}\text{Sc}-\beta^+$  decays, either directly to the 1524-keV  $2^+$  level or to the 2423-keV  $2^+$  level which cascades through the 1524-keV state about 50% of the time, have been estimated by DelVecchio and Daehnick<sup>12</sup> to be at least five orders of magnitude smaller than the branch of Eq. (9b). In any event, such transitions are not accompanied by a 313-keV  $\gamma$  ray and would be rejected by the NaI(Tl) filter. The contribution, following the second-order reaction  $^{42}\text{Ca}(n, p)$ , from  $^{42}\text{K}$  which  $\beta^-$  decays to the 1524-keV level in  $^{42}\text{Ca}$  some 18% of the time was estimated by Ingalls, Overley, and Wilson<sup>11</sup> to be negligible. Furthermore, the fast decay of the 1524-keV line evident in Figs. (4a) and (4b) is not consistent with the 12.4-h half-life of  $^{42}\text{K}$ .

#### VI. DISCUSSION

Our value for the branching ratio in Eq. (9b) overlaps, within error estimates, that of Ingalls, Overley, and Wilson,<sup>11</sup>  $(6.2 \pm 2.6) \times 10^{-5}$ . It is, however, significantly different from that of DelVecchio and Daehnick<sup>12</sup> who obtained  $(2.2 \pm 1.7) \times 10^{-5}$ . Since the square of the Fermi matrix element is inversely proportional to the  $ft$  value, BR is just the product of  $\delta_1$ , as defined in Eq. (1), and the ratio (0.148) of phase-space factors for the transitions to the 1837-keV and ground states of  $^{42}\text{Ca}$ .<sup>5</sup> Our value of BR from Eq. (9b) implies

$$\delta_1 = (6.9 \pm 2.0) \times 10^{-4} \quad (10a)$$

(this measurement).

Towner has used a simple Coulomb-mixing model to estimate  $\delta_1$  for  $^{42}\text{Sc}$  decay. Using the wavefunctions of Gerace and Green<sup>19</sup> and a perturbative approach to the mixing of the ground and first excited  $0^+$  states in  $^{42}\text{Sc}$

and  $^{42}\text{Ca}$ , Towner predicted<sup>5</sup>

$$\delta_1 = 4.5 \times 10^{-4} \quad (10b)$$

(weak-coupling estimate).

This value is very near our lower limit in Eq. (10a). However, Towner has noted a large cancellation between two terms in the calculation of  $\delta_1$  that results in a high degree of sensitivity to the wave functions used. More extensive large-basis shell-model calculations by Towner,<sup>5</sup> using the Rochester-Oak Ridge Code, have led to estimates of

$$\delta_1 = 18.9 \times 10^{-4} \quad (10c)$$

(shell model+ CF),

with  $T_3$ -dependent mixing generated by the Coulomb force (CF), and

$$\delta_1 = 15.5 \times 10^{-4} \quad (10d)$$

(shell model+ CF + CDNF),

with the additional inclusion of a charge-dependent nuclear force (CDNF). In still another large basis shell-model calculation, Towner and Hardy<sup>4</sup> included all known  $0^+$  states in  $^{42}\text{Ca}$  and  $^{42}\text{Sc}$ , rather than confining the mixing to the  $0^+$  levels nearest the ground states, and obtained

$$\delta_1 = 13 \times 10^{-4} \quad (10e)$$

(shell model+ CF + CDNF + mixing into all  $0^+$  levels).

However, it should be remembered that this latter value of  $\delta_1$  gives only an upper limit for the mixing of the  $^{42}\text{Ca}$  ground state into the excited  $0^+$  level at 1837 keV, and is not simply related to the branching ratio of Eq. (9b) as are the estimates of Eq. (10b), (10c), and (10d). The microscopic shell model calculations overestimate  $\delta_1$  by at least a factor of 2, and the importance of this discrepancy is evident when these values are compared to the estimates<sup>3</sup> for the radial overlap correction  $\delta_2$ , as defined in Sec. I:

$$\delta_2 = (36 \pm 3) \times 10^{-4} \quad (10f)$$

(shell model).

[The error in Eq. (10f) reflects the variation in  $\delta_2$  that results from choosing different wave functions.] The results of attempts<sup>2</sup> to obtain nucleon-structure information from the difference between the coupling constants of  $\beta$  decay

and muon decay are sensitive to the corrections  $\delta_1$  and  $\delta_2$  and, for the most part, shell model calculations have been used to estimate these. However, in the case of  $^{42}\text{Sc}$  decay our deduced value of  $\delta_1$  is only 19% of the estimates for  $\delta_2$ . Unfortunately, the high degree of sensitivity to the model wave functions, encountered by Towner<sup>5</sup> in the calculation of  $\delta_1$  for mass 42, prevents drawing general conclusions for other nuclei on the relative importance of  $\delta_1$  vs  $\delta_2$ .

In retrospect, the experimental techniques involved in our measurement were quite complicated and it became difficult to keep all facets of the experiment properly functioning at the same time. Consequently, large blocks of data were discarded in preparing this paper with the result that our reliable data shown in Fig. 4, although having a much better peak-to-background ratio than previous measurements,<sup>11,12</sup> still have poor statistics in the peak of interest. There are, however, modifications to this experiment that would greatly improve the statistics of the 1524-keV peak. Tests above the  $^{42}\text{Sc}^{7+}$  threshold showed that the detection system described in Sec. II could function properly at much higher counting rates than were actually used, and targets three to four times thicker than those used in this work would multiply the data of Fig. 4 correspondingly. A similar result could also be obtained by simply increasing the time devoted to the experiment. Furthermore, measurements with the Ni foil in front of the rabbit replaced by a 5.5-mg/cm<sup>2</sup> Ta foil removed the 1332- and 1790-keV lines from Fig. 3 and reduced the long-lived background in the vicinity of 1524 keV by about 30%. If theoretical calculations evolve to the state of being sensitive to the error limits of the present work, or those of Ingalls *et al.*,<sup>11</sup> it may be worth repeating this measurement. We believe that the experimental techniques described here are capable of reducing the error on BR to the level of a few percent.

#### ACKNOWLEDGMENTS

We would like to thank D. H. Wilkinson for his keen interest during the early stages of this experiment. This work was supported by the U. S. Department of Energy under Contract No. DE-AC02-76CH00016.

<sup>1</sup>R. J. Blin-Stoyle, in *Isospin in Nuclear Physics*, edited by D. H. Wilkinson (North-Holland, Amsterdam, 1969).

<sup>2</sup>D. H. Wilkinson, in *Nuclear Physics with Heavy Ions and Mesons*, edited by R. Balian (North-Holland, Amsterdam, 1978); *Nature* **257**, 189 (1975).

<sup>3</sup>I. S. Towner, J. C. Hardy, and M. Harvey, *Nucl. Phys.*

**A284**, 269 (1977).

<sup>4</sup>I. S. Towner and J. C. Hardy, *Nucl. Phys.* **A205**, 33 (1973).

<sup>5</sup>I. S. Towner, *Phys. Lett.* **43B**, 267 (1973).

<sup>6</sup>P. M. Endt and C. Van der Leun, *Nucl. Phys.* **A310**, 1 (1978).



- <sup>7</sup>J. M. Freeman, D. C. Robinson, G. Murray, and W. E. Burcham, A. E. R. E. Nucl. Phys. Div. Prog. Report No. PR/NP13 (1968).
- <sup>8</sup>G. T. Garvey, K. W. Jones, D. Schwalm, and E. K. Warburton, Phys. Lett. 35B, 563 (1971).
- <sup>9</sup>H. J. Kennedy and J. D. McCullen, Phys. Rev. Lett. 27, 198 (1971).
- <sup>10</sup>W. E. Burcham, G. Murray, D. C. Robinson, J. M. Freeman, and J. E. Jenkins, Proc. R. Soc. Edinburgh A70, 4 (1971/1972).
- <sup>11</sup>P. D. Ingalls, J. C. Overley, and H. S. Wilson, Nucl. Phys. A293, 117 (1977).
- <sup>12</sup>R. M. DelVecchio and W. W. Daehnick, Phys. Rev. C 17, 1809 (1978).
- <sup>13</sup>D. R. Goosman and D. E. Alburger, Phys. Rev. C 5, 1252 (1972); 6, 825 (1972); G. E. Schwender, D. R. Goosman, and K. W. Jones, Rev. Sci. Instrum. 43, 832 (1972).
- <sup>14</sup>A. M. Sandorfi (unpublished).
- <sup>15</sup>J. B. Gerhart, B. C. Carlson, and R. Sherr, Phys. Rev. 94, 917 (1954).
- <sup>16</sup>F. Ajzenberg-Selove, Nucl. Phys. A300, 1 (1978).
- <sup>17</sup>E. J. Kobetich and R. Katz, Phys. Rev. 170, 391 (1968); M. J. Berger and S. M. Seltzer, Nat. Advis. Comm. Aeronaut. Report No. SP-3012 (1964).
- <sup>18</sup>M. Ulrickson, W. Hartwig, N. Benczer-Koller, J. R. MacDonald, and J. W. Tape, Phys. Rev. C 13, 536 (1976).
- <sup>19</sup>W. J. Gerace and A. M. Green, Nucl. Phys. A93, 110 (1967).